EUROPEAN FUSION DEVELOPMENT AGREEMENT

EFDA–JET–PR(02)04

P. Maget et al

# Statistical Analysis of Internal Transport Barriers in JET

# Statistical Analysis of Internal Transport Barriers in JET

P. Maget[1], B. Esposito[2], E. Joffrin[1], N. Hawkes[3], D. Mazon[1],
Y. Baranov[3], C. Fourment[1], G.T. Hoang[1]
and contributors to the EFDA-JET workprogramme*

*[1]Association Euratom-CEA, Cadarache, F-13108 St Paul-lez-Durance, France*
*[2]Associazione Euratom-ENEA sulla Fusione, C.R. Frascati, Fracati, Italy*
*[3]Euratom-UKAEA Fusion Association, Culham Science Centre, Abingdon, Oxon, OX14 3DB, UK*
**See annex of J. Pamela et al, "Overview of Recent JET Results and Future Perspectives", Fusion Energy 2000 (Proc. 18th Int. Conf. Sorrento, 2000), IAEA, Vienna (2001).*

Paper to be submitted for publication in Nuclear Fusion

**ABSTRACT**

Internal Transport Barriers (ITB) in JET exhibit some remarkable features regarding their relation toward the shearing rate and the current profile. A database has been collected over a large number of pulses, and focuses on some specific plasma parameters at the barrier location : the gradient lengths, safety factor (q), magnetic shear (s), and shearing rate ($\gamma_E$). In the present work, we analyse the database in two different perspectives. First, we address the question of the shearing rate and its two contributions, i.e. toroidal rotation and diamagnetic term : we find that the plasma toroidal rotation is the dominant term, the diamagnetic contribution being estimated from the neoclassical drive. A correlation between the velocity shear rate and the magnetic shear is found, in agreement with previous works, and a minimum is seen at low magnetic shear. The definition of ITB as a departure from profile stiffness is compared to the use of the JET ITB criterion, and both approaches are found to be consistent. Second, we address the question of the barrier localisation in relation to the safety factor and the magnetic shear. We find that barriers are sensitive to rational q surfaces, as far as their location and performance are concerned. In reversed shear plasmas, obtained by applying current drive during the plasma ramp up, ITB can also be sustained in the negative shear region, where integer values of the safety factor does not seem to play a role.

The paper is organised in four sections : in section 1 it is explained how the database has been built; the error bars on the safety factor and magnetic shear are evaluated in section 2; then comes in section 3 the analysis of the shearing rate and its relation to the magnetic shear; in section 4, we discuss the relation between the safety factor and the magnetic shear at the barrier position; a conclusion follows.

## 1. PRINCIPLE OF THE DATABASE

The database covers a total of 139 pulses (from JET experiments) for which Internal Transport Barriers were produced. First, the inverse gradient length of the temperature is calculated in the electron (from ECE data) and ion (from charge exchange spectroscopy) channels. The gradient length is defined by $L_x \equiv -X/\nabla X$, where the gradient is performed against the toroidal flux co-ordinate. The later is linked to a distance, by analogy with the cylindrical circular case.

The radial position of the barrier is assumed to be at the point of maximum $1/L_T$. Several points are taken during the pulse in both the electron and ion channels, in order to cover as much as possible the range of plasma conditions for which the Internal Transport Barrier can exist. Note that electron and ion channels are investigated separately, and this is done for several reasons. First, a barrier can be detected in one channel and not in the other. Second, the radial location of the barrier is not always consistent in both channels. Also, some problems on the calculation of $1/L_T$ can be encountered in one case and not in the other at a given time and/or radius. By doing so, we deliberately exclude the direct comparison of co-existing electron and ion barriers.

In order to be consistent with a recent criterion for the ITB detection in JET (Tresset et al., [1]), the quantity $\rho_T^* \equiv 0.00457 \sqrt{T_e^{keV}}/(|B|L_T)$ is calculated. Note that this criterion, although similar in spirit to the one used by Tresset et al., is based on a different radial derivative, the major radius

being replaced by the toroidal flux co-ordinate. The use of such a quantity to qualify the strength of a barrier have shown its usefulness in our study, since barriers are not always associated with a triggering event, as is often defined the transition to an ITB. The question of barrier definition and barrier triggering can be avoided by considering such a parameter, the transition to the ITB domain being replaced by an adjustable threshold in $\rho_T^*$. For experimental purpose, the threshold on JET (with the derivative relative to the major radius) was estimated around 0.014 during the 2001 campaign for the real-time control of ITBs [2]. The separation of different ranges in $\rho_T^*$ in the following of this paper will cover the different possible appreciation of the level at which an ITB is present.

At the points thus defined in the ($R$,$t$) space, where $R$ is the major radius and $t$ the time, several quantities are calculated : the safety factor and the magnetic shear given by the equilibrium code EFIT, with or without the Motional Stark Effect (MSE) or polarimetry (POL) constraint, and the shearing rate (see section 3). The reconstruction with MSE has been taken into account only when the radial electric field correction was available. A linear interpolation in ($R$,$t$) space is made to determine these quantities at the required radius and time. In figure 1 are shown the inverse gradient lengths in the electron and ion channels for a particular pulse, together with the points that have been recorded in the database, indicated by the stars.

## 2. SAFETY FACTOR & MAGNETIC SHEAR: DETERMINATION & UNCERTAINTIES

The magnetic equilibrium is calculated with the EFIT code, whether with the constraint of magnetic loops only (“standard” calculation, hereafter referred to as STD), or with the additional constraint of the Motional Stark Effect (MSE), or polarimetry (POL) diagnostics. When the MSE signal is available, it yields important information on the central part of the plasma, especially when the current profile is hollow. Reconstructions constrained by polarimetry are also able to identify hollow current profiles. During the last campaigns, Lower Hybrid Current Drive (LHCD) during the current ramp-up (preheat phase) has been extensively used, leading to extreme reversed shear plasmas that were revealed by the MSE diagnostic [3]. A broad range of current profiles have been tested towards transport barrier production by this mean, as reported in [4]. The standard EFIT run is unable to reconstruct these strongly reversed q profiles, and shows instead a large flat central q region. However, the standard reconstruction provides a correct result at larger radii.

Despite its usefulness in analysing reversed shear plasmas, MSE reconstructions are subject to specific constraints. Indeed, due to the degradation of the MSE signal when all the neutral beams are used, we sometimes rely on two equilibriums only for deriving the safety factor profile during the time of interest : one just before the main heating phase, and the other just after. A linear interpolation has been made to determine the safety factor and magnetic shear at the time and location required, which may induce some distortion in the data.

With the constraint of polarimetry, we benefit from the contribution of the core plasma current along the line of sight. However, its weight in the equilibrium reconstruction is less than with a

local measurement as MSE, and this will tend to smooth strongly reversed profiles. Also, the information about the current profile is mixed to the electron density profile in the Faraday rotation signal.

There are other aspects to consider for the question of accuracy. Because of the different spatial resolution of ECE and charge-exchange diagnostics, it is necessary to separate both channels when addressing the question of safety factor and magnetic shear, for which a good localisation is a precious advantage. Apart from the question of the magnetic equilibrium reconstruction, the accuracy on the localisation of the barrier becomes more crucial as we deal with higher magnetic shear regions, where the safety factor varies rapidly. As a consequence, we expect better results in the electron channel (better spatial resolution), whereas at large magnetic shear, the situation is balanced between the inconvenient of the rapid variation of the safety factor ($\Delta q/q \equiv s\,\Delta r/r$) and the advantage of a more constrained reconstruction with magnetic loops.

In order to estimate the order of magnitude of the error bars, especially on the safety factor, we have chosen to compare these quantities when they can be determined by the three different equilibrium reconstructions. Only part of the database benefit from this multiple evaluation of the current density profile. We have separated pulses without (figure 2a) and with (figure 2b) LH power in the preheat phase, on the hypothesis that equilibrium reconstruction may be more difficult in situations where a hollow plasma current exist. Each point corresponds to the average on the three reconstruction, and the error bars are delimited by the maximum and minimum values. In both figures, the error bars on the safety factor are large in the low and negative magnetic shear region, except when q is below 1.5. In the higher magnetic shear region, the error bars on the safety factor is generally less than 0.3, except for q above 2.5. Concerning the magnetic shear, error bars are quite large in the domain s>1 but large discrepancies exist also for q>2.5.

## 3. SHEARING RATE

The calculation of the shearing rate relies on the estimation of the radial electric field, which is not a straightforward quantity to determine. Having no systematic direct measurement of the poloidal rotation, we assume that it follows the neoclassical approximation: $V_{\theta,i}^{neo} \sim -k_{neo}\,\nabla T_i/(Z_i B)$ where $Z_i$ is the atomic charge of the ion, and $k_{neo}$ is a coefficient depending on the ion species and the regime of collision. The radial electric field is then given by:

$$E_r = V_{\varphi,i} B_\theta - \frac{T_i}{Z_i}\left[\frac{1}{L_{n,i}} + \frac{1 + k_{neo}}{L_{T,i}}\right]$$

and the shearing rate is :

$$\gamma_E \approx \frac{(RB_\theta)^2}{B}\,\frac{d}{d\psi}\,\frac{E_r}{RB_\theta}$$

where $B_\theta$ is the poloidal magnetic field, and $\psi$ is the poloidal magnetic flux. Following the decomposition of the radial electric field in a term linked to the toroidal rotation and a term related

to diamagnetic frequencies, we will refer to a decomposition of the shearing rate into a toroidal rotation term and a diamagnetic term.

We have made several assumptions in order to perform the calculation of the radial electric field. First, we assume that the effective atomic charge of the plasma ($Z_{eff}$) is constant over the radial domain of the barrier, so that the electron density profile from the LIDAR diagnostic can be used for the calculation of the ion density gradient length. The only impurity is assumed to be carbon. It is from the spectral analysis of carbon radiation that the charge-exchange diagnostic calculates the angular rotation and ion temperature. We have therefore a consistent estimate of the shearing rate by calculating $k_{neo}$ for carbon. However, these assumptions are not valid in cases where impurities accumulate inside the ITB, leading to a peaked $Z_{eff}$ profile. Such an accumulation of impurities was indeed observed during some JET ITBs [5], and this could lead to a contribution of density gradient stronger than what we calculate. The neoclassical term $k_{neo}$ for carbon is determined from a comprehensive calculation of trapped particle fraction and using the viscosity coefficients from [6]. Whereas it is about -1.17 for deuterium in the banana regime, it is over -1 for carbon, so that temperature gradient contribution adds to the density gradient contribution. This coefficient increases with the collision frequency, and eventually becomes positive. With these assumptions, we have plotted the ratio of the diamagnetic term to the total shearing rate (figure 3). It appears that the diamagnetic component is not the dominant contribution to the shearing rate that we calculate. As the shearing rate becomes larger, the diamagnetic contribution becomes negligible. At least can we conclude that this is true at the spatial resolution that is made possible by the diagnostic (~10 cm). More localised variations of the velocity shear have indeed be reported at the ITB triggering in TFTR [7] and ASDEX-UPGRADE [8], and a mechanism such as mode coupling could explain such behaviour [9]. But so far, it is not supported by direct experimental evidence on JET.

An interesting point is that the toroidal rotation of carbon follows closely the carbon temperature in JET. Because most of the experiments are performed with a similar torque from the neutral beams, and because of the similar diffusivity of momentum and ion energy (reported in [10] and [11] for example), the shear in toroidal rotation and the ion temperature gradient are closely related. This is illustrated in figure 4, where a restriction has been made on the time variation of the diamagnetic energy, in order to rule out the points recorded during the transitory period of spinning up of the plasma. The consequence is that the shearing rate is linked to the ion temperature gradient in a quasi formal way, whatever the role of the shearing rate in the sustainement of the ion barrier.

The results of the database can also be related to a recent work on the link between the shearing rate and the magnetic shear at the formation of ITBs [12]. By plotting the shearing rate (normalised to $v_{Ti}/R$ where $v_{Ti}$ is the ion thermal velocity and R the major radius of the plasma), as a function of the magnetic shear at the place and moment of the ITB formation for a series of pulses, the authors had found that the normalised shearing rate was an increasing function of the magnetic shear. This observation can be tested against our database, which includes barriers at negative magnetic shear, not covered in ref. [12]. By taking into account the ITB criterion, we include also a quantitative

parameter in the definition of an ITB. In Ref. 12, the pulses that were studied exhibit a very clear transition to the ITB, which is not always the case in the pulses covered by our database (see Fig. 1 as an example). For this reason, the use of the ITB criterion is crucial for qualifying the existence of a barrier. What we find for ion barriers (figure 5) is that the frontier of the ITB domain, which is interpreted here as an iso-$\rho_T^*$ curve, is indeed an increasing function of the magnetic shear in the s>0 part of this ($\gamma_E R/v_{Ti}$ ,s) diagram. The frontier defined in Ref. 12 is consistent with the threshold $\rho_T^* \approx 0.015$ used on JET experiments. Unfortunately, we have only few points from MSE and POL reconstruction in the range $\rho_T^* > 0.015$. A minimum in $\gamma_E R/v_{Ti}$ can be inferred at low magnetic shear, the negative magnetic shear domain being covered by EFIT reconstructions with MSE or polarimetry. It suggests that the shearing rate associated to the transition to the ITB domain is lower in the low magnetic shear region. Note however that, in contrast with the empirical frontier determined in Ref. 12, this minimum value does not seem to go to zero at low or negative magnetic shear.

Another approach to which our database can bring some input is the definition of transport barriers in relation to a critical value of $R/L_T$, as done for JET and ASDEX in [13,14,15], and DIII-D in [16]. From this point of view, it is the departure from strongly resilient profiles, close to the critical $R/L_T$, that is interpreted as the presence of a barrier. This alternative approach for the definition of a transport barrier relies on the theory of micro-instabilities such as Ion Temperature Gradient (ITG), Trapped Electron (TEM), or Electron Temperature Gradient (ETG) modes. Numerous studies, experimental as well as theoretical, have mentioned a dependence of this critical gradient upon the magnetic shear and/or the safety factor. A sheared slab ITG model yields a dependence $(R/L_{Ti})_c = 1.88\ |s|/q\ (1+Z_{eff}\ T_i/T_e)$ [17], and a similar result was found for ETG modes [18]. Toroidal effects introduce an offset, as observed in [19] for ITG turbulence, and gyrokinetic simulations of toroidal turbulence driven by the ETG modes yield $(R/L_{Te})_c = (1.33+1.9\ s/q)\ (1+Z_{eff}\ T_e/T_i)$ [20]. However, magnetic shear and safety factor are expected to be independent parameters in toroidal geometry, and recent gyrokinetic calculations of linear stability tend to find more complicated expressions, but they indicate a minimum at low magnetic shear for the critical gradient of ITG as well as ETG modes [21]. For practical purpose, these expression have been fitted using only the variable s/q, which gives:

$$\begin{cases} (R/L_{Te})_c/(1 + Z_{eff}\ T_e/T_i) = 2.2 - 4.6s/q & s < 0 \\ \qquad\qquad\qquad\qquad\quad = 2.1 + 3.4s/q & s > 0 \end{cases}$$

$$\begin{cases} (R/L_{Ti})_c/(1 + T_e/T_i) = 1.4 - 12s/q & s < 0 \\ \qquad\qquad\qquad\quad = 1.6 + 4s/q & s > 0 \end{cases}$$

Note that these expression are not valid at vanishing magnetic shear.

From the experimental point of view, it has been found in Tore Supra Hot Electron experiments that the critical gradient was following a dependence on s/q : $(R/L_{Te})_c = 5(\pm1)+10(\pm2)\ s/q$ [22], which is consistent with the above expression within error bars.

Following this approach, we have calculated these quantities throughout the database. Figure 6 shows the result for electron barriers (figure 6a) and ion barriers (figure 6b). The critical value, as

determined above, is also drawn on these figures. In the electron channel, the lower limit of the domain covered by the database follows rather well the critical value, in both the positive and negative magnetic shear region, the latter being described by the MSE and POL reconstructions only. The relation to the ITB criterion appears also clearly : the criterion is low (typically less than 0.01) close to the critical value, and it increases above it. In the ion channel, this relation between the ITB criterion and the normalised gradient given in ordinate is also convincing, but the dependence on s/q seems weaker. The observation of a critical value is reminiscent of the positive offset on figure 5.

We find therefore that the concept of transport barrier, from a practical point of view, can be defined whether from the ITB criterion, or from the idea that profile stiffness is overcome.

## 4. SAFETY FACTOR AND MAGNETIC SHEAR : ANALYSIS OF THE DATABASE

We examine the relation between the safety factor and the magnetic shear at the barrier position. The ITB criterion will be used as an indication of the ITB strength. A useful discrimination between the large number of points is obtained by separating experiments with and without LHCD in the preheat. We will therefore examine 4 sets of figures (figure 7 to 10) by separating ion and electron barriers, and experiments with and without LHCD preheat. Each set of figures contains the result obtained from EFIT standard reconstruction, from MSE reconstruction, and from POL reconstruction.

From these (s,q) plots, it appears that the safety factor and magnetic shear play a role in the localisation of the barrier, since points are organised along well identified structures. It is in the electron channel that these structures are the more apparent, because of the better radial localisation of the barrier. In this channel, we observe (figure 7) that experiments without LHCD preheat exhibit a remarkable concentration of points around integer values of the safety factor, for a large range of magnetic shears. The largest cluster is around q=2, but barriers localised close to q=1 and q=3 are also represented. A cluster of points around q=2.5 with lower performance is also visible in figure 7a. MSE and POL data covers only part of the data set. In these series (figures 7b and 7c), the q≈2 branch is found at a lower value. This can be understood by the fact that the higher central q value detected by MSE and POL reconstructions shifts the external rational surface outwards. From a physical point of view, it would imply that the barrier is located inside the q=2 surface.

In the ion channel, and still without LH preheat, the structures are broader, but still present around q=2 and q=3 when looking at the standard reconstruction plot (figure 8a). MSE and POL series (figures 8b and 8c) do not cover the highest performance pulses. As can be seen from a comparison between figures 7a and 8a, similarities can be seen found in electron and ion barriers, but the spatial resolution in the ion channel is probably too poor to identify structures in the (s,q) plot.

For LHCD preheated plasmas, we observe both similarities and differences (figures 9 and 10). At positive magnetic shear, we recognise clearly a branch around q=2, covering a large range of magnetic shears, and confirmed with MSE or POL reconstructions. A similar branch exists around q=3 in the POL reconstruction. In the ion channel, we can recognise by comparison these two structures, but the points are more scattered.

But the results suggest that another kind of barrier may exist, characterised by a low magnetic shear (figures 9 and 10). This appears as a "vertical" structure in the negative magnetic shear domain in MSE and POL reconstructions of figure 9, showing that LHCD preheat gives access to negative magnetic shear barriers. Integer safety factor surfaces, for these barriers, seems unimportant. Errors bars in the negative shear domain are of course quite large, but even when considering a single reconstruction, there seem to be no clusters of points around particular values of the safety factor. These plots support the idea that some values of the safety factor, close to integers, are privileged in monotonic q profile experiments. They reflect previous observations that Internal Transport Barriers in JET seemed to be linked to rational values of the safety factor [23]. An important role of the safety factor is however not clearly supported by theoretical works on the subject, except around the s=0 surface [24]. At present time, most works on anomalous transport outline the role of the magnetic shear, whether through the zero magnetic shear surface, or through the negative magnetic shear region [24,25]. This role can be reinforced by the Shafranov shift [26]. The importance of reversed magnetic shear configurations in the ITB formation has indeed been shown by many authors [27, 4, 28], and the discussion about the ITB frontier as a function of the magnetic shear (section 3) supports the idea that this parameter is essential. But another mechanism must be invoked for the relation to the safety factor. The insertion of more macroscopic phenomenon such as MHD modes could be a lead for explaining the particular role of integer safety factor surfaces in non zero magnetic shear regions, as suggested for the ITB triggering in [29].

## 5. CONCLUSION

Our statistical analysis of JET Internal Transport Barriers is addressing the questions of shearing rate, barrier strength and barrier localisation in relation to the safety factor and magnetic shear. We find that the shearing rate of ExB flow is dominated by the toroidal rotation of the plasma, in the hypothesis that poloidal rotation is governed by its lowest order neoclassical estimate. Because of this, the calculated shearing rate and the ion temperature gradient follow the same behaviour, whatever their possible indirect link through turbulence suppression. We have also been able to compare our results to previous works concerning the possible link between the shearing rate (or the temperature gradient) to the magnetic shear at the frontier of ITB domain. We confirm the increase of the shearing rate with the magnetic shear already found for JET ITBs in the positive shear domain, and we extend this result in the negative shear domain. Another definition of ITBs, based on the departure from profile stiffness, is compared to the use of the ITB criterion. We find that these approaches are compatible and that the dependence on s/q predicted by theory and found experimentally on Tore Supra is also true for JET electron barriers.

On the question of barrier localisation, we find strong indications, from three different reconstructions of the magnetic equilibrium, that low order rational values of the safety factor play a role in the localisation of the barrier, especially in the positive shear region. When LHCD is used in the preheat phase, a negative magnetic shear region is created in the centre, and transport barriers

are also observed in this region. These barriers do not exhibit a clear preference for particular safety factor surfaces, as far as we can observe from the present analysis. In these reversed shear plasmas, barriers can also exist in the positive magnetic shear region, and tend to localise close to rational safety factor surfaces.

**AKNOWLEGMENTS**

This work has been conducted under the European Fusion Development Agreement. Particular thanks are due to X. Garbet for his encouragements and his critical reading, as well as for fruitful discussions.

**REFERENCES**

[1]. TRESSET, G., et al., Nuclear Fusion**42** (2002), 520

[2]. MAZON,D., et al., Real-time control of internal transport barriers in JET, submitted to Plasma Phys. Control. Fusion (2002)

[3]. HAWKES, N., et al., Physical Review Letters **87** (2001), 115001

[4]. CHALLIS C.D., et al., Plasma Phys. Control. Fusion **43** (2001), 861

[5]. DUX, R., et al.., Proc. of the 28th EPS Conference on Controlled Fusion and Plasmas Physics **25A**, Madeira (2001), P2.007

[6]. KESSEL, C.E., Nuclear Fusion **34** (1994), 1221

[7]. BELL, M., et al., Plasma Phys. Control. Fusion **41** (1999), A719

[8]. DE PENA HEMPEL, S., et al., 25$^{th}$ EPS Conf. on Controlled Fusion and Plasmas Physics, Praha, **22C** (1998), 484

[9]. JOFFRIN, E., et al., 27$^{th}$ EPS Conf. on Controlled Fusion and Plasmas Physics, Budapest, **24B** (2000), 237

[10]. DE ESCH, H.P.L., et al., Proc. 17$^{th}$ EPS Conf. on Controlled Fusion and Plasmas Physics I (Amsterdam, Holland) (1990), 90

[11]. SCOTT, S.D., et al., Physical Review Letters **64** (1990), 531

[12]. TALA, T.J.J.,HEIKKINEN, J.A., PARAIL, V.V., BARANOV, Y.F., KARTTUNEN, S.J., Plasma Phys. Control. Fusion **43** (2001), 507

[13]. WOLF, R.C., et al., Proc. of the 28th EPS Conference on Controlled Fusion and Plasmas Physics **25A**, Madeira (2001), 513

[14]. TARDINI, G., et al., Nuclear Fusion **42** (2002), 258

[15]. PEETERS, A.G., et al., Proc. of the 18th IAEA Conference, Fusion Energy, Sorrento, Italy, October 2000, (CD-Rom) ( IAEA, Vienna, 2001) , IAEA-CN-77/EXP5/06

[16]. BAKER, D.R., et al., Physics of Plasmas **8** (2001), 4128

[17]. HAHM, T.S., and TANG, W. M., Phys. Fluids B 1, 1185 (1989)

[18]. HORTON,W., et al., Physics of Plasmas **7** (2000), 1494

[19]. DIMITS, A.M. et al., 18th International Atomic Energy Agency Fusion Energy Conf., IAEA-CN-77/THP1/03 (2000)
[20]. JENKO, F., W. DORLAND, and G. W. HAMMETT, Physics of Plasmas **8** (2001), 4096
[21]. FOURMENT, C., et al., Role of The Current Density Profile On Drift Wave Stability In Internal Transport Barrier Reversed Magnetic Shear Experiments At JET And Tore Supra, to be published (2002)
[22]. HOANG, G.T., et al., Physical Review Letters **87** (2001), 125001-1
[23]. COTTRELL, G.A., et al., Plasma Phys. Control. Fusion **40** (1998), 1251
[24]. KISHIMOTO, Y., et al., Nuclear Fusion **40** (2000), 667
[25]. GARBET, X., et al., Physics of Plasmas **8** (2001), 2793
[26]. BEER, M.A., et al., Physics of Plasmas **4** (1997), 1792
[27]. ERIKSSON, L.G., et al., Physical Review Letters **88** (2002), 145001-1
[28]. ESPOSITO, B., et al., Proc. of the 28th EPS Conference on Controlled Fusion and Plasmas Physics **25A**, Madeira (2001), 553
[29]. JOFFRIN, E.,CHALLIS, C.D., HENDER, T.C., HOWELL, D.F., HUYSMANS, G.T.A., Nuclear Fusion **42** (2002), 235

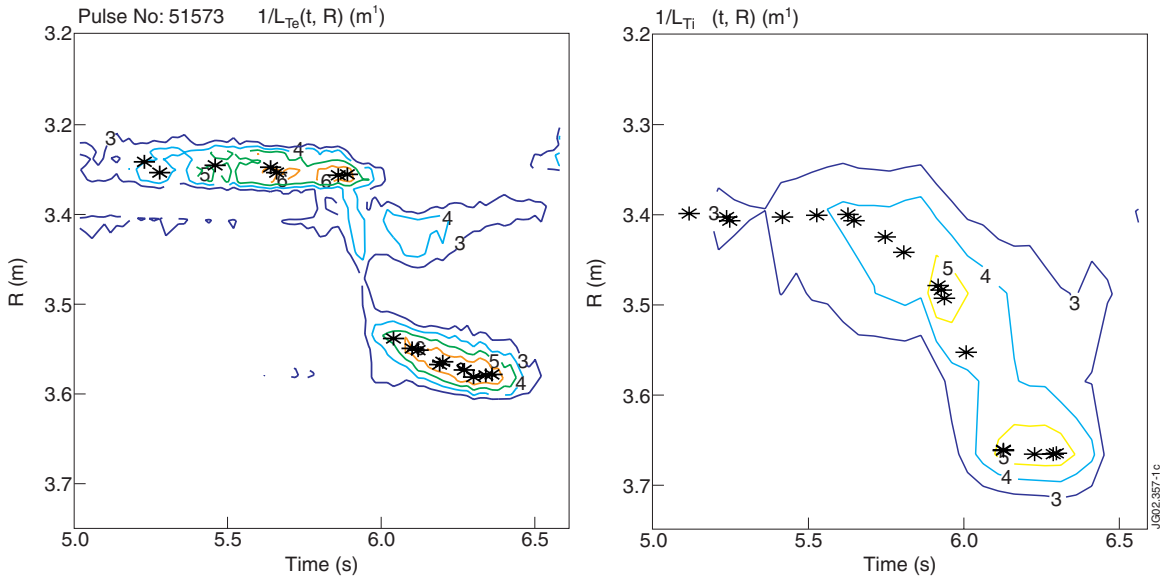


*Figure 1: Inverse temperature gradient length for electrons (left) and ions (right) as a function of time and major radius (Pulse No: 51573). The stars indicate the points selected in the database.*

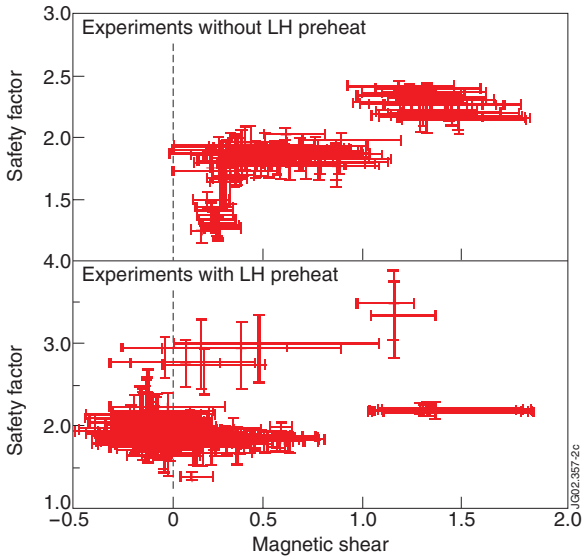


*Figure 2: Error bars on magnetic shear and safety factor determined from points having the 3 reconstructions available. Experiments without (up) and with (down) LH in the preheat phase.*

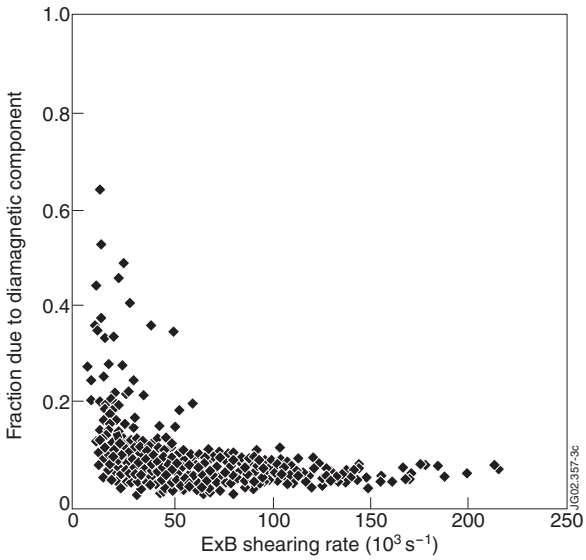


*Figure 3: Fraction of the diamagnetic contribution to the total shearing rate, as a function of the total ExB shear, for the ion barriers.*

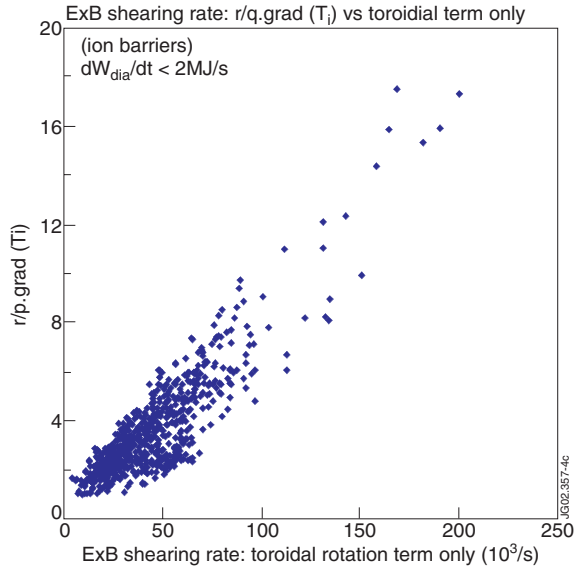


*Figure 4: Comparison of the flow shear and ion temperature gradient : r/q grad($T_i$) is plotted against r/q grad ($V_{\phi i}$/R).*

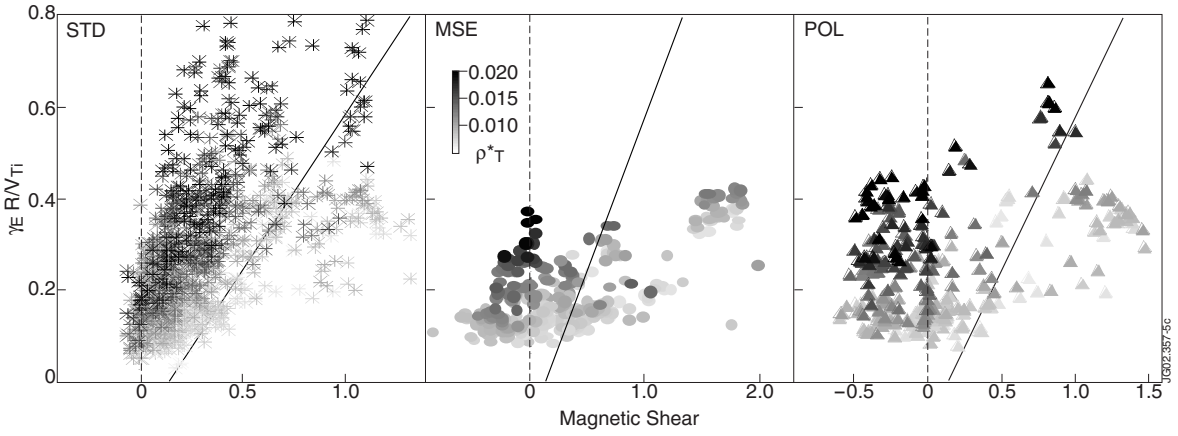


*Figure 5: Normalised shearing rate as a function of the magnetic shear given by the 3 reconstructions (STD, POL, MSE). The grey scale is related to the ITB criterion. The line is the frontier of the ITB domain as determined in Ref. 12.*

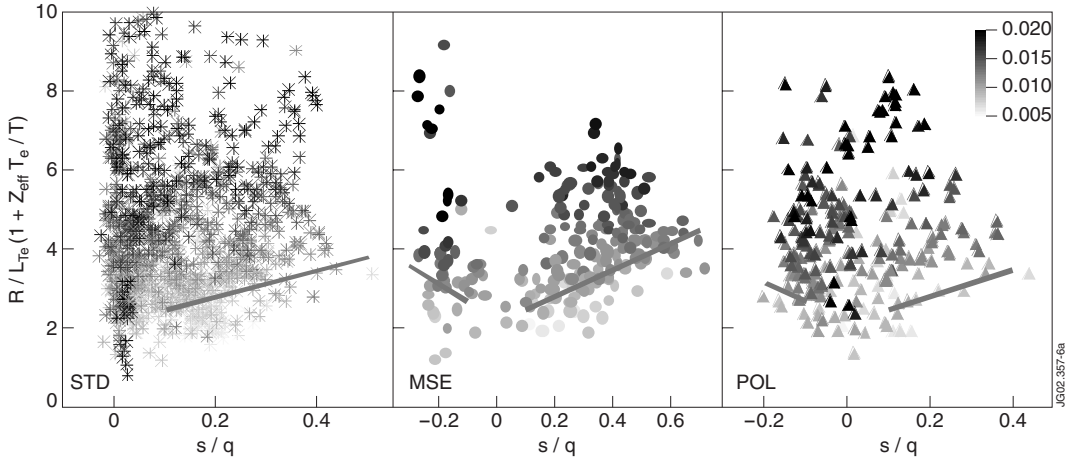


*Figure 6a: $R/L_{Te}$ normalised as indicated in the text, as a function of s/q, given by the 3 reconstructions (STD, POL, MSE). The grey scale is related to the ITB criterion. The line corresponds to the critical normalised $R/L_T$.*

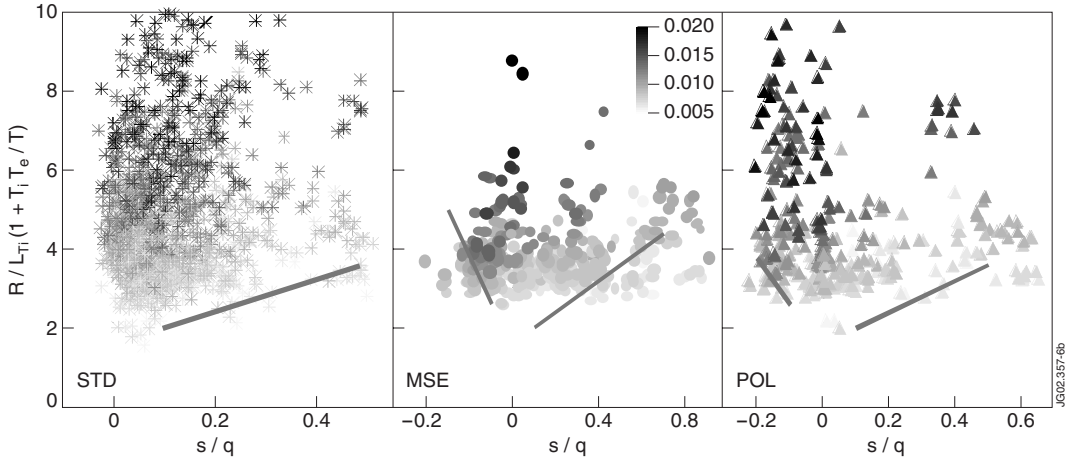


*Figure 6b: $R/L_{Ti}$ normalised as indicated in the text, as a function of s/q, given by the 3 reconstructions (STD, POL, MSE). The grey scale is related to the ITB criterion. The line corresponds to the critical normalised $R/L_T$.*

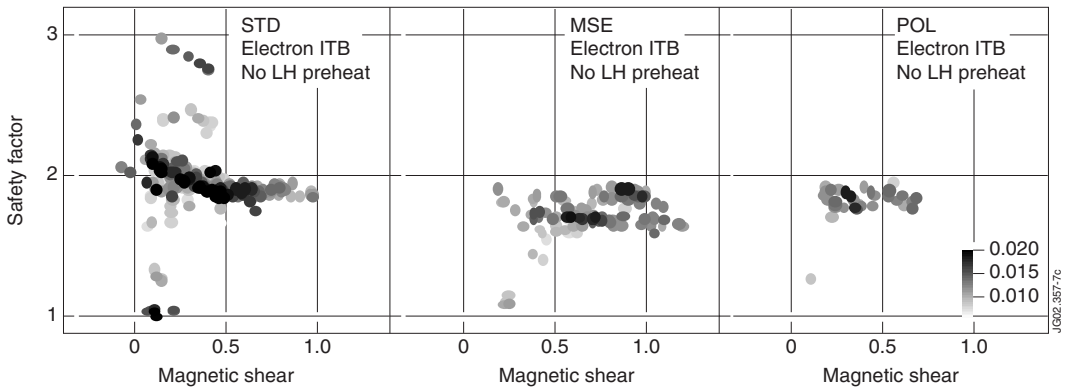


*Figure 7: Safety factor versus magnetic shear, for electron barriers without LH preheat.*

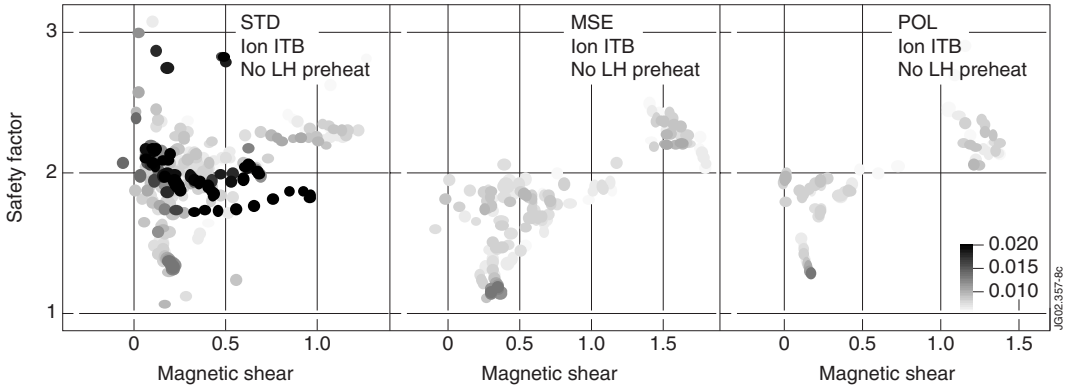


*Figure 8: Safety factor versus magnetic shear, for ion barriers without LH preheat.*

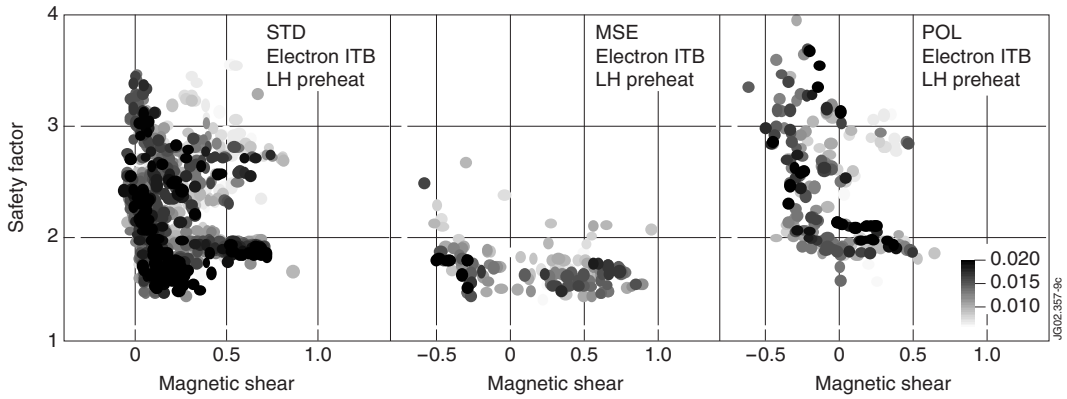


*Figure 9: Safety factor versus magnetic shear, for electron barriers with LH preheat.*

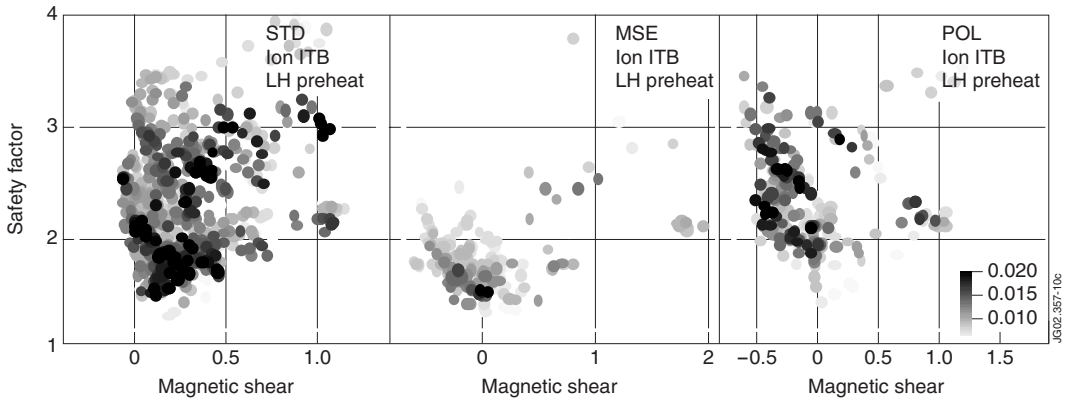


*Figure 10: Safety factor versus magnetic shear, for ion barriers with LH preheat.*